Molecular Composition and Photochemical Evolution of Water Soluble Organic Carbon (WSOC) Extracted from Field Biomass Burning Aerosols using High Resolution Mass Spectrometry

Jing Cai[1,2], Xiangying Zeng[1], Guorui Zhi[3], Sasho Gligorovski[1], Guoying Sheng[1], Zhiqiang Yu[1,*], Xinming Wang[1], Ping'an Peng[1]

[1]*State Key Laboratory of Organic Geochemistry, Guangdong Key Laboratory of Environment and Resources, Guangzhou Institute of Geochemistry, Chinese Academy of Sciences, Guangzhou, 510640, China*

[2]*University of Chinese Academy of Sciences, Beijing, 100049, China*

[3]*State Key Laboratory of Environmental Criteria and Risk Assessment, Chinese Research Academy of Environmental Sciences, Beijing, 100012, China*

*corresponding author: Dr. Zhiqiang Yu

Tel: +86-13728068752

Fax: +86-20-85290288

E-mail: zhiqiang@gig.ac.cn

ABSTRACT

Photochemistry plays an important role in the evolution of atmospheric water soluble organic carbon (WSOC), which dissolves into clouds, fogs and aerosol liquid water. In this study, we tentatively examined the molecular composition and evolution of a WSOC mixture extracted from field-collected wheat straw burning aerosol (WSBA) samples upon photolysis, using direct infusion electrospray ionization (ESI) coupled to high-resolution mass spectrometry (HRMS) and liquid chromatography (LC) coupled with HRMS. For comparison, two typical phenolic compounds (i.e., phenol and guaiacol) emitted from lignin pyrolysis in combination with hydrogen peroxide (H_2O_2) as a typical OH radical precursor were simultaneously exposed to simulated sunlight irradiation. Their photochemical products such as phenolic dimers (e.g., m/z 185.0608 for phenol dimer and m/z 245.0823 for guaiacol dimer) or their isomers, were also observed in field-collected WSBA samples, suggesting that the aqueous-phase reactions might contribute to the formation of emitted biomass burning aerosols. The aqueous photochemistry of both the phenols (photooxidation) and WSBA extracts (direct photolysis) could produce a series of highly oxygenated compounds which in turn increases the oxidation degree of organic composition and acidity of the bulk solution. In particular, the LC/ESI-HRMS technique revealed significant photochemical evolution of the WSOC composition in WSBA samples, e.g., the photodegradation of low oxygenated species and the formation of highly oxygenated products. We also tentatively compared the mass spectra of photolytic time-profile WSBA extracts with each other for a more comprehensive description of the photolytic

evolution. The calculated average oxygen-to-carbon ratio (O/C) of oxygenated compounds in bulk extract increases from 0.38±0.02 to 0.44±0.02 (mean±standard deviation) while the intensity (S/N)-weighted average O/C (O/C_w) increases from 0.45 ±0.03 to 0.53±0.06 as the time of irradiation extends from 0 to 12h. These findings indicate that the water soluble organic fraction of combustion-derived aerosols has the potential to form more oxidized organic matter, contributing to the highly oxygenated nature of atmospheric organic aerosols.

1 INTRODUCTION

Water-soluble organic carbon (WSOC) comprises a significant fraction of atmospheric aerosols, accounting for 20–80% of total organic carbon (OC) (Krivacsy et al., 2001; Wozniak et al., 2008; Fu et al., 2015; Xie et al., 2016). WSOC is directly involved in the formation of cloud condensation nuclei (CCN) by modifying the aqueous chemistry and surface tension of cloud droplets (Graham et al., 2002; Nguyen et al., 2012; Zhao et al., 2013; McNeill 2015). Despite its significance, little is known about the chemical composition and sources of WSOC, with less than 10–20% of the organic mass being structurally identified (Cappiello et al., 2003; Fu et al., 2015). Biomass burning is a well-known emission source of WSOC (Anastasio et al., 1997; Fine et al., 2001; Graham et al., 2002; Mayol-Bracero et al., 2002; Gilardoni et al., 2016). Although the composition varies with fuel type and combustion conditions (Simoneit 2002; Smith et al., 2009), the WSOC mixture often covers a common range of polar and oxygenated aromatic compounds (Graham et al., 2002; Mayol-Bracero et al., 2002; Duarte et al., 2007; Chang and Thompson 2010; Yee et al., 2013; Gilardoni

et al., 2016) with molecules incorporating different numbers of functional groups like hydroxyl, carboxyl, aldehyde, ketone, ester, amino and/or other nitrogen-containing groups (Graham et al., 2002). In particular, lignin pyrolysis often yields a large amount of aromatic alcohols, carbonyls, and acid compounds (Mayol-Bracero et al., 2002; Chang and Thompson 2010; Gilardoni et al., 2016). Once dissolved into cloud, fog, and even aerosol liquid water, these substances can undergo aqueous-phase reactions to generate low-volatility species under sunlight irradiation, which have the potential to form secondary organic aerosol (SOA) after water evaporation (Graham et al., 2002; Cappiello et al., 2003; Duarte et al., 2007; Sun et al., 2010; Yu et al., 2014).

Field and laboratory studies have demonstrated that aqueous photochemical processes contribute significantly to the aqueous SOA formation from biomass burning precursors and the evolution of smoke particles (Sun et al., 2010; Lee et al., 2011; Kitanovski et al., 2014; Yu et al., 2014; McNeill 2015; Gilardoni et al., 2016). Gilardoni et al. (2016) observed aqueous SOA formation in both fog water and wet aerosols, resulting in an enhancement in the oxidized OA, and following atmospheric aging the overall oxidation degree of aerosols has also increased. In laboratory studies, phenols and methoxyphenols (important biomass burning intermediates) are often used as SOA precursors to examine the photochemical evolution in aqueous environments and aerosol-forming potential under relevant atmospheric conditions (Chang and Thompson 2010; Sun et al., 2010; Smith et al., 2014; Yu et al., 2014; Vione et al., 2019). The corresponding photochemical products formed through hydroxylation, oligomerization, and fragmentation typically cover a series of low-volatility and highly

oxygenated species. For instance, the methoxyphenol-derived SOA are proposed as a proxy for atmospheric humic-like substances (HULIS) (Ofner et al., 2011; Yee et al., 2013). Other compounds emitted from lignin pyrolysis, e.g., aromatic alcohol, carbonyl, and carboxylic species retaining the phenyl ring have also been found to produce colored products via aqueous photooxidation, which may become a part of HULIS (Chang and Thompson 2010; Huang et al., 2018). In addition, photochemical processing of common water-soluble aliphatic compounds such as aldehydes (Lim and Turpin 2015), polyols (Daumit et al., 2014), and organic acids (Griffith et al., 2013) in aqueous solution can also lead to the formation of oligomers, highly oxygenated and multifunctional organic matter (McNeill 2015).

In recent years, high resolution mass spectrometry (HRMS) has been commonly applied to study the organic molecular composition in cloudwater (Zhao et al., 2013; Boone et al., 2015), fogwater (Cappiello et al., 2003), rainwater (Altieri et al., 2009a; Altieri et al., 2009b), laboratory-generated SOA (Bateman et al., 2011; Romonosky et al., 2015; Lavi et al., 2017), and field-collected aerosol samples (Laskin et al., 2009; Lin et al., 2012a; Lin et al., 2012b; Kourtchev et al., 2013; Tong et al., 2016; Wang et al., 2017). It has also been used in time-profile observations of the photochemical evolution of aqueous extracts from laboratory-generated SOAs (Bateman et al., 2011; Romonosky et al., 2015). However, direct infusion MS methods are prone to ion suppression caused by other organic species, inorganic salts, and adduct formation (Kourtchev et al., 2013). Therefore, liquid chromatography (LC) coupled with HRMS might be another complementary powerful tool for relieving ion suppression due to its

abilities to separate and analyze different kind of compounds with differences in LC retention time (Kourtchev et al., 2013; Wang et al., 2016). It could also provide more information enabling the identification of possible isomers from the ions with same mass-to-charge ratio (m/z).

To our knowledge, the aqueous photochemical evolution of WSOC extracted from real ambient aerosols has not been studied in detail at the molecular level. Our previous study has revealed that the ultraviolet-visible (UV-VIS) absorption spectra of aqueous extracts from field biomass burning aerosols were modified under simulated sunlight illumination (Cai et al., 2018). Based on the previously studied field-collected samples, the present study is focused on a further analysis to investigate the molecular characteristics of water-soluble organic molecules by the photochemical evolution using electrospray ionization (ESI)-HRMS and LC/ESI-HRMS performed in negative ionization mode. For comparison, we also evaluated the photochemistry of phenol and guaiacol (representing the basic structures of phenols emitted from lignin pyrolysis) under laboratory conditions, and tentatively traced some of their photochemical products (e.g. dimers) in field-collected samples under study.

2 EXPERIMENTAL SECTION

2.1 Particulate sample collection and preparation of aqueous extracts

The wheat straw burning aerosol (WSBA) samples were collected during the summer harvest season of 2013, at rural fields in the plain of north China where the wheat was the main agricultural crop (Cai et al., 2018). To facilitate subsequent planting and

management, a large amount of fresh wheat straw was directly burned in the field during the harvest season, and the water emitted from burning plant body could provide a suitable environment for aqueous photochemistry of dissolved compounds. The selected WSBA samples used for HRMS analysis were collected from two sampling sites, located at rural fields in Wenxian in Henan Province (noted: HNWX) and Daming in Hebei Province (HBDM). As described in Cai et al. (2018), the selected sampling sites were mainly affected by heavy smog from wheat straw burning (Figure 1). The emitted fine particulate matter with aerodynamic diameter $\leqslant$2.5μm ($PM_{2.5}$) was collected at a flow rate of 5 L min^{-1} by a portable particulate sampler (MiniVol TAS, AirMetrics, USA), with quartz fiber filters (47mmin diameter, QMA, Whatman, UK) baked at 600°C for 6 hours before sampling. The sampling flow rate was calibrated with a standard flow meter (Bios Defender 520) and the sampling time of each filter was restricted to 30-60 minutes depending on the ambient biomass burning aerosol concentration and expected filter loading (Cai et al., 2018). After collection, the filter samples were stored in dark and transported to the laboratory, and then stored at -20°C under a light-proof condition.

The preparation of WSOC extracts and measurements for carbon content including organic carbon (OC), elemental carbon (EC) and WSOC were described in detail in Cai et al. (2018). Briefly, a part of each quartz fiber filters (1.6-3.2 cm^2) was placed into a brown vial and extracted with ultra-pure water (Milli-Q, Milipore) for two times; at each time 5 ml ultra-pure water with a 30 min ultrasonic agitation was applied. The two-time extracts were combined and filtered through a PTFE syringe filter (0.2 μm

pore size, Thermo Scientific), followed by a pH measurement with a pH meter (Mettler Toledo SevenEasyTM S20) that has been regularly calibrated at pH 4.00 and 6.86. Prior to analysis the extracts were stored at -20°C in the dark. To reduce the WSOC mass loss, the desalting treatment (e.g., solid phase extraction (SPE)) was not performed on these samples.

Figure 1. One field site at Daming, Hebei province, China, for sampling the aerosols affected by biomass burning.

2.2 Direct photolysis of WSOC extracts

A 12-hour direct photolysis of WSOC extracts obtained from WSBA samples was performed in a photo-reactor (BL-GHX-V, Bilon Instruments Co. Ltd., China, see Figure S1) that was equipped with a solar simulator (Xe lamp, 1000W) placed into a double-deck quartz condenser (Cai et al., 2018). A cooling water (18°C) was circulating in the outer tube of the condenser to avoid heating of the samples. In the wavelength range of 310-400 nm relevant to the boundary layer of the atmosphere, the actinic flux

of the lamp is about 5 times stronger than the solar actinic flux, meaning that the spectral evolution via the 12-hour simulated solar irradiation might be equal with the effect caused by actual sunlight irradiation with a duration of at least 60 hours (Cai et al., 2018). Air-tight quartz tubes (1.5cm in diameter, 3ml solution per tube) loading extracts were equidistantly arranged around the lamp. Each extract was distributed into three tubes that corresponded to three different irradiation times, i.e. 0, 4, and 12 h, with no oxidants added externally throughout the whole photolytic process. At each irradiation time point (e.g., 0 and 4 h), the related tubes were wrapped with aluminum foil, and placed at the initial location until the end of 12-h photolysis (Cai et al., 2018).

As described in Cai et al. (2018), the water extraction resulted in a dilution of the collected organic compounds, however, the ratio of the water mass to $PM_{2.5}$ mass for extract samples (ranging from 1.8×10^3 to 3.4×10^4) was compatible with the ratio of water mass to WSOC content in cloud water (in a wide range from 1.4×10^2 to 1.6×10^4) (Li et al., 2017), indicating that the present aqueous extracts are relevant to the atmospheric cloud water condition.

2.3 Photooxidation of phenolic compounds under laboratory conditions

Initial solutions of 0.1 mM phenol (C_6H_6O) and 0.1 mM guaiacol ($C_7H_8O_2$) in combination with an OH radical precursor (0.1 mM H_2O_2) were prepared in ultra-pure water (Milli-Q, Milipore). The pH of the solution was adjusted to 5 with 0.1 M sulfuric acid (H_2SO_4), which is usually relevant to the acidity in fog and cloud waters (Collet et al., 1998; Fahey et al., 2005). The prepared solution and reference blank were irradiated by simulated sunlight irradiation with a duration of 4 hours. Hereby, we mainly focus

on acquiring the chemical characteristics of aqueous products of phenols, and tentatively identify some tracer compounds (e.g., phenolic dimers) whether they exist in present biomass burning particulate samples.

2.4 Sample analysis

The direct infusion MS analysis was conducted using a Thermo Scientific Orbitrap Fusion Tribrid mass spectrometer equipped with quadrupole, orbitrap, and linear ion trap mass analyzers, with a heated ESI source. To assist in ionization and desolvation, the sample was diluted to a 1:1 mixture of acetonitrile and sample by volume. The full scan mass spectra were acquired in negative ionization mode, with a resolution of 120000 at *m/z* 200 for the Orbitrap analyzer and a mass scan range of m/z 50-750. Before determination, the Orbitrap analyzer was externally calibrated for mass accuracy using Thermo Scientific Pierce LTQ Velos ESI calibration solution. The direct infusion parameters were as follows: sample flow rate 5 μl min^{-1}; capillary temperature 300°C; S-lens RF 65%; spray voltage -3.5 kV; sheath gas, auxiliary gas, and sweep gas flows were 10, 3, and 0 arbitrary units, respectively. Data collecting was performed when the intensity of the total ion current (TIC) maintained constant with a relative standard deviation (RSD) under 5%. At least 100 data points (mass spectral scans) were collected for each test sample, and the each exported mass spectrum for analysis was derived from the average result of 100 spectrums.

The LC/ESI-HRMS analysis operated in negative ionization mode was performed using a U3000 system coupled with a T3 Atlantis C18 column (3 μm; 2.1×150 mm; Waters, Milford, USA) and an Orbitrap Fusion MS. A 10 μL sample was injected, with

a flow rate of 0.2 ml min^{-1} for the mobile phase, which consisted of H_2O (A) and acetonitrile (B). The gradient applied was 0-5 min 3% B; 5-20 min from 3 to 95% (linear), and kept for 25 min at 95%; and 45-50 min from 95 to 3%, and held for 10 min at 3% (total run time 60 min).

2.5 Data processing

Mass spectral peaks with three times larger than the signal to noise ratio (S/N) were extracted from the raw files. Peaks in both sample and blank spectra were retained if their intensity in the former was five times larger than in the latter. A common molecular assignment based on the accurate mass was performed using Xcalibur software (V3.0 Thermo Scientific) with the following constraints: $^{12}C \leq 50$, $^{13}C \leq 1$, $^{1}H \leq 100$, $^{16}O \leq 50$, $^{14}N \leq 4$, $^{32}S \leq 1$, and $^{34}S \leq 1$. All mathematically possible elemental formulas, with a mass tolerance of ±3ppm were calculated. Elemental formulas containing ^{13}C or ^{34}S were checked for the presence of ^{12}C or ^{32}S counterparts, respectively. If they were not matched with the corresponding monoisotopic formulas, then the assignment with next larger mass error was considered. Isotopic and unassigned peaks were excluded from further analysis.

Ions were also characterized by the number of rings plus double bonds (i.e., double bond equivalents (DBE)), which were calculated as: $DBE = c - h/2 + n/2 + 1$ for an elemental composition of $C_cH_hO_oN_nS_s$. The assigned formula was additionally checked with the nitrogen rule. For ambient samples, based on the presence of various elements in a molecule, the identified elemental formulas were classified into several main compound classes: CHO (i.e., molecules containing only C, H, and O atoms), CHOS,

CHON, and CHONS, and others including CHN and CHS. In the present study, because the detected water-soluble ions almost were below m/z 400, we focused our molecular analysis on m/z 50-400.

3 RESULTS AND DISCUSSION

3.1 Mass spectral characteristics of WSOC extracts from WSBA samples

The preliminary analysis showed that the $PM_{2.5}$ concentration in ambient air near to the burning sites ranged from 6.46 to 28.03 mg m^{-3} (Table S1). OC was the major component of the collected $PM_{2.5}$ with a proportion of 50.9±7.6% (mean±standard deviation), whereas EC represented a negligible fraction (average 1.3 ± 0.4%). Meanwhile, WSOC accounted for 35.5±7.5% of OC in the tested samples.

Although this batch of aerosol samples were collected from different sites, their water-extracted solutions showed similar light-absorbing characteristics in UV-VIS absorption spectra (Cai et al., 2018). Here, four extract samples (HNWX-1, HNWX-2, HBDM-1 and HBDM-2) (Table S1) were chosen for further analysis using high resolution mass spectrometry. These samples also exhibited similar patterns in mass distribution of water-soluble molecular species that mainly range from 50 to 400 Da, which indicated a similar burning source for these samples. A reconstructed mass spectrum (subtracted blank) for one representative sample of HNWX-1 is shown in Figure 2a (others are shown in Figure S2). In mass range 50-400 Da, there were 827± 44 molecular formulas identified throughout the all samples, and most of the formulas (above 75%) were overlapped between these analyzed samples. The classification features of assigned compounds for analyzed extracts are shown in Table S2. In the

amount of assigned formulas, CHO composition was the most abundant group, accounting for 59.2±2.2% of the total assignments, followed by CHON (35.0±2.2%). These results are consistent with previous observations of laboratory-generated biomass burning aerosol (Smith et al., 2009) and field particulate samples influenced by biomass combustion (Kourtchev et al., 2016) in spite of the differences of biomass varieties, extracted solvents, and HRMS techniques between present and previous studies.

On the other hand, CHOS and CHONS compounds contributed with less than 5% to the total assignment. A number of studies have shown the wide presence of organosulfates and nitrooxy-organosulfates in urban (Lin et al., 2012b; Wang et al., 2016), rural (Lin et al., 2012a), and forest aerosols (Kourtchev et al., 2013), and even in cloudwater (Boone et al., 2015); however, most of these compounds were not observed in our negative mass spectra. This could be accounted for by the low extent of aerosol evolution, due to the limited oxidation conditions available for the formation of organosulfates and nitrooxy-organosulfates in fresh smoke aerosols. For example, laboratory studies have observed the significant formation of organosulfates via photooxidation in the presence of acidic sulfate aerosol (with significant level of SO_2 concentration) (Surratt et al., 2007; Surratt et al., 2008). All detected ion species with enabled formula assignments in present samples are listed in Table S3. In general, CHN and CHS compounds are not ionized well in negative ESI mode, which could be a reason why these species were not the most prevalent compounds in this study.

It should be also noted that the negative ionization mode selectively targets to detect those molecules containing polar functional groups (e.g., -OH and –COOH) that could

be readily deprotonated. There are number of compounds that are not easily deprotonated and might show up preferentially in positive ionization mode (e.g., amines). Furthermore, the formula numbers detected in the HRMS potentially contain multiple structural isomers; therefore, the actual number of water-soluble organic species is expected to be underestimated. The additional LC/ESI-HRMS analysis operated in negative mode confirmed a substantial number of ion masses (e.g., assigned CHO and CHON compounds) containing more than one structural isomer, which could be observed at different retention times (RTs) in chromatograms. Two representative groups of extracted chromatograms for CHO ($[C_7H_5O_n]^-$, (n=2~4)) and CHON ($[C_7H_5O_nN]^-$, (n=1~3)) compounds are shown in Figure S3 and S4, respectively, where increasing the O or N atom number in a molecule might lead to more isomer peaks. However, it should be noted that these LC-separated peaks might also include other unidentified compounds that were outside of the elemental assignment considered in this study. Additionally, low mass loading and potential decomposition under the ionization can also limit the detection of some high molecular weight species.

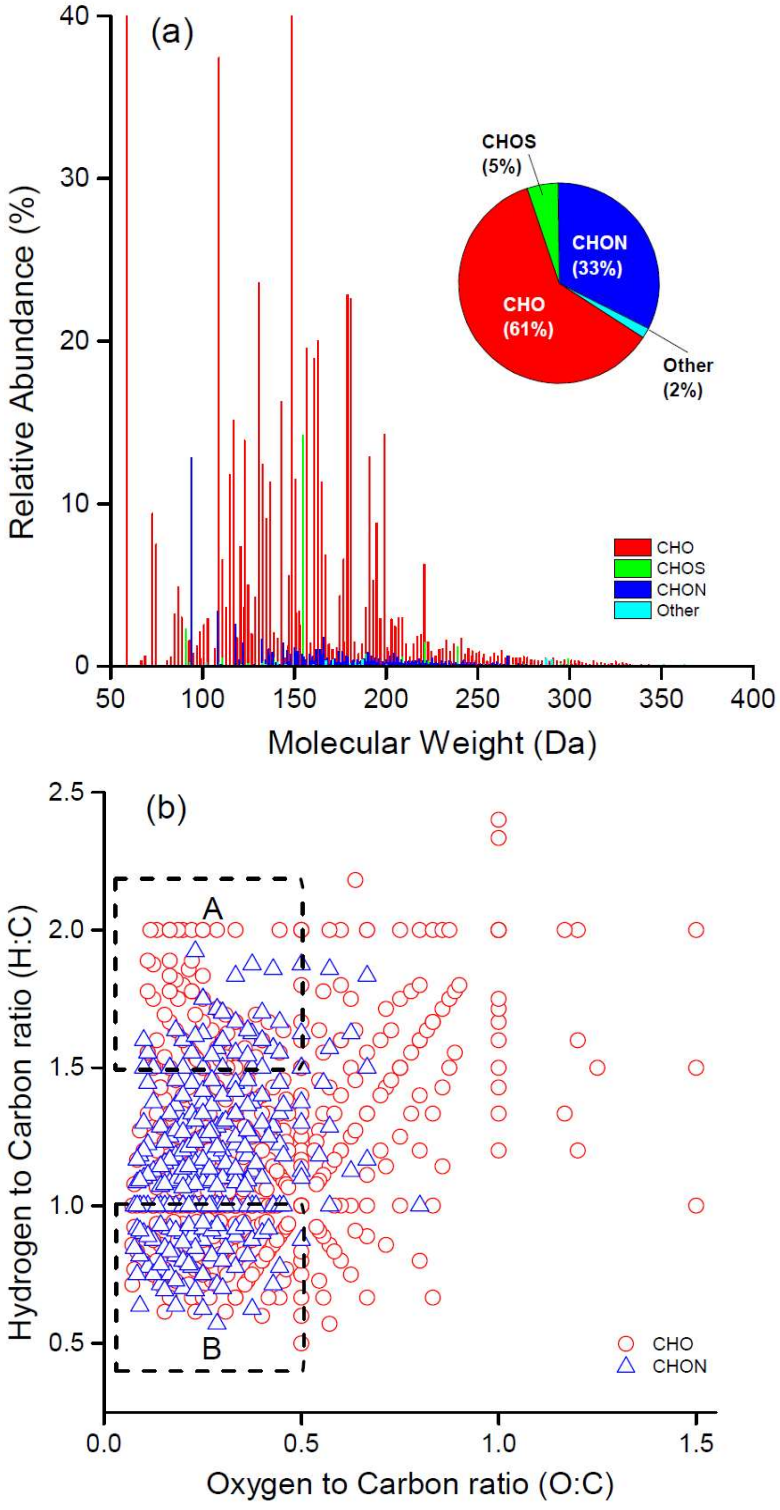

Figure 2. (a) Reconstructed mass spectra for detected ions with assigned formulas and (b) Van Krevelen diagrams for CHO and CHON species in extract of HNWX-1 sample. The inset pie charts in (a) show the number fraction of each class in the total assigned compounds. Areas A and B in (b) are tentatively attributed to aliphatic and aromatic species, respectively.

303 The interpretation of the complex organic mass spectra generated by high resolution
304 mass spectrometry can be simplified by plotting the hydrogen to carbon ratio (H/C)
305 against the oxygen to carbon ratio (O/C) for individual assigned atomic formulas in
306 form of the Van Krevelen (VK) diagram (e.g. Lin et al., 2012a; Kourtchev et al., 2013).
307 Figure 2b indicates a representative VK diagram of CHO and CHON compounds
308 derived from HNWX-1 sample. It can be clearly seen from Figure 2b that the majority
309 of CHO and CHON molecules are located at the region of O/C$\leqslant$1.0 and H/C$\leqslant$2.0. In
310 VK diagram, molecules with H/C$\leqslant$1.0 and O/C$\leqslant$0.5 are typical for aromatic species,
311 while molecules with H/C$\geqslant$1.5 and O/C$\leqslant$0.5 would be associated with typical
312 aliphatic compounds (Mazzoleni et al., 2012; Kourtchev et al., 2014). The average
313 double bond equivalent (DBE) showed relative high values with 5.5 for CHO
314 compounds and 6.1 for CHON compounds (Table S2), suggesting that unsaturated
315 organic species were abundant in present samples, and their presence could partially
316 account for the strong light-absorbing feature in the near-UV region as observed in our
317 previous study (Cai et al., 2018).
318 Throughout the extract samples, the average H/C and O/C values were ranging from
319 1.26±0.38 to 1.31±0.40 and from 0.34±0.24 to 0.42±0.29 for CHO compounds, and
320 from 1.19±0.32 to 1.23±0.35 and from 0.28±0.17 to 0.29±0.15 for CHON compounds
321 (Table S2), respectively. Although the ESI analysis were performed in the negative
322 ionization mode, the measured O/C exhibit rather low values, which fall in the range of
323 O/C ratios typical for biomass burning organic aerosol derived from positive ionization
324 mode (Aiken et al., 2008; Kourtchev et al., 2016). Due to fresh emission and smaller

aging effect, the present O/C were obviously lower than the O/C of long-range transport biomass burning aerosols (Zhang et al., 2018).

Carbon oxidation state (OS_c) was observed to increase with oxidation for atmospheric organic aerosol and link strongly to aerosol volatility (Kroll et al., 2011). OS_c for each molecular formula can be calculated using the following equation:

$$OS_c = -\sum_i OS_i \frac{n_i}{n_c}$$

where OS_i is the oxidation state associated with non-carbon element i and n_i/n_C is the molar ratio of element i to carbon within the molecule (Kroll et al., 2011; Kourtchev et al., 2013).

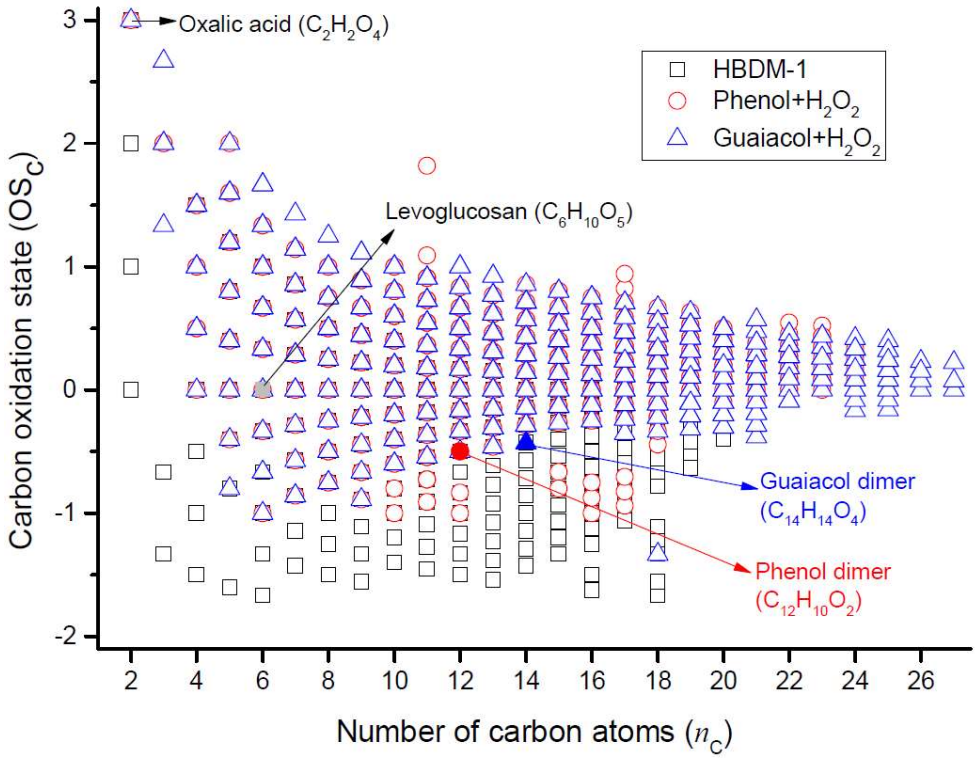

Figure 3. The distribution of carbon oxidation state (OS_C) for CHO molecules in HBDM-1 and laboratory samples produced from phenol and guaiacol photooxidation in presence of H_2O_2 (i.e., Phenol+ H_2O_2 and Guaiacol+ H_2O_2). The locations of oxalic acid (identified in HBDM-1 and laboratory samples), levoglucosan (identified in HBDM-1), phenol dimer (identified in Phenol+ H_2O_2), guaiacol dimer (identified in Guaiacol+ H_2O_2) are shown.

Considering that nitrogen and sulfur atoms can present multiple oxidation states, the OSc was calculated and analyzed only for CHO compounds in this study. A similar pattern of OSc values versus the number of carbon atoms (n_C) was observed for CHO compounds detected in present WSBA samples (Figure 3 and Figure S5). From Figure 3 and Figure S5, it can be seen that OSc of each sample ranges mainly from -1.5 to +1 with average ranging from -0.6 to -0.4. Consistent with previous studies (Kroll et al., 2011; Kourtchev et al., 2016), the majority of molecules with $OS_C < 0$ (low oxidized organics) and carbon atoms lower than 20 are suggested to be associated with the primary organic aerosols emitted from biomass burning. A minor fraction of molecular formulas with $OS_C \geq 0$ values might be associated with semivolatile and low-volatility oxidized organic aerosols (Kroll et al., 2011). Figure 3 also shows the plot of OS_c versus n_C for products obtained from photooxidation of phenol and guaiacol, respectively, and their comparison with WSBA samples will be discussed in section 3.3.

3.2 Mass spectral characteristics of the products from photooxidation of phenolic compounds in the aqueous phase

Phenol and guaiacol were chosen as two representative model compounds derived from biomass combustion. Two high resolution mass spectra of aqueous phenol and guaiacol exposed to OH radicals for 4h are shown in Figure S6, where 435 $C_xH_yO_z$ molecular formulas (m/z 90-500) were assigned for product ions of phenol (with C_3-C_{24}) and 624 $C_xH_yO_z$ formulas (m/z 90-600) were assigned for product ions of guaiacol (with C_3-C_{27}). The average H/C and O/C values were 0.79 ± 0.28 and 0.52 ± 0.23 for phenol, and 0.88 ± 0.24 and 0.59 ± 0.24 for guaiacol, respectively. Clearly, the

photochemical processing induced by OH oxidation resulted in an increase in average O/C of product molecules relative to their precursors (O/C = 0.17 for phenol and O/C= 0.29 for guaiacol).

The formation mechanisms of series of oxygenated products, e.g., phenolic oligomers, hydroxylated phenolic species, ring-opening and highly oxygenated compounds, are proposed in the literature (e.g. Sun et al., 2010; Chang and Thompson, 2010; Yu et al., 2014; Huang et al., 2018). The OH-initiated reactions would result in enhanced hydroxylation of the aromatic ring as well as in increased yields of carboxylic acids and toxic dicarbonyl compounds (Sun et al., 2010; Yu et al., 2014; Prasse et al., 2018). For example, some highly oxygenated C_2-C_5 aliphatic compounds (e.g., $C_2H_2O_4$, $C_3H_4O_4$, $C_4H_6O_4$, and $C_5H_6O_5$) corresponding to carboxylic acids (Yu et al., 2014) were clearly observed in the mass spectra of present photochemical products. The occurrence of these oxygenated products not only directly increased the degree of oxygenation in the bulk solution composition, but also contributed to the variation of solution acidity. After the 4-hours photochemical process, the pH values of the irradiated solution were significantly lower than the pH values of the solution prior to irradiation (t-test, p <0.05), and the calculated acidities ($[H^+]$) of the bulk solution increased by $(2.96 \pm 0.15)\times10^{-5}$ M and $(4.26 \pm 0.16)\times10^{-5}$ M for phenol and guaiacol, respectively.

The oligomerization induced by photochemical transformation of phenolic substances is an important formation pathway for low-volatility, light-absorbing compounds (Smith et al., 2016). Here, phenolic dimmers (i.e., $C_{12}H_{10}O_2$ for phenol dimer and $C_{14}H_{14}O_4$ for guaiacol dimer) and higher oligomers (e.g., $C_{18}H_{14}O_3$ and

384 $C_{24}H_{18}O_4$ for phenol trimer and tetramer, $C_{21}H_{20}O_6$ for guaiacol trimer), as well as their
385 hydroxylated species were observed. The formation mechanism can be ascribed to C-
386 O or C-C coupling of phenoxy radicals that were formed via H-abstraction of the
387 phenols or OH addition to the aromatic ring (Net et al., 2009, Sun et al., 2010). The
388 reaction at the para position or para-para coupling was more likely to occur due to a
389 higher probability of free electron to occur in this position (Lavi et al., 2017) or a weaker
390 steric hindrance in the para position.

391 **3.3 Comparison of the photochemical products of phenolic compounds and the**
392 **CHO composition in WSOC extracts from WSBA samples**

393 Compared to the CHO compounds detected in WSOC extracts, the photochemical
394 products of the two phenols under study showed a higher O/C and a lower H/C values.
395 The average OS_C of photochemical products from phenol (OS_C = -0.7) and guaiacol
396 (OS_C = -0.6) after a 4-hour photooxidation raised to +0.2 and +0.3, respectively,
397 showing distinctly a higher degree of oxidation than the present WSBA samples. In
398 Figure 3, more species with $OS_C < 0$ (especially $OS_C < -0.5$) are presented in the field
399 sample (HBDM-1), while the species with $OS_C \geqslant 0$ are prevalent in photochemical
400 products of phenol and guaiacol. The single-precursor systems in laboratory did not
401 completely reflect the CHO composition features in water-soluble extracts from real
402 straw-burning samples that contained a myriad of precursors and unknown substances
403 from atmospheric background, soil and other sources. Considering that a large number
404 of phenols and methoxyphenols exist in the straw-burning smokes and their potential
405 to undergo photochemical aging, the nature of emitted primary organic aerosols is

406 reasonably more complicated than the nature of simulated products derived from single-
407 precursor systems.

408 The extracted LC chromatograms of m/z 185.0608 and 245.0823 are shown in Figure
409 4, respectively, where both ions involve dimers of phenol and guaiacol with several
410 structures, and/or other isomers. The presence of guaiacol dimer and syringol dimer
411 was previously observed in aerosol samples largely affected by wood combustion.
412 Based on the Aerosol Mass Spectrometer (AMS) analysis, these two dimers were
413 suggested as markers of biomass burning aerosols (Sun et al., 2010; Yu et al., 2014). In
414 the composition of present biomass burning aerosols, the phenolic dimers (m/z
415 185.0608 and 245.0823) were also observed in present mass spectra, but the extracted
416 LC chromatograms shown in Figure 4 indicate that these ions contain multiple RT peaks.
417 The same peaks with RT18.3 and 19.2 min which are assumed to be the phenol dimers
418 were observed during the photochemical transformation of phenol (Figure 4a) and in
419 the WSBA samples. Meanwhile, the present particle extracts may also involve guaiacol
420 dimer, since its m/z 245.0823 has two LC peaks emerged at RT 17.7 and 19.5 min
421 (Figure 4b) same as the peaks identified during the photochemical transformation of
422 guaiacol. Considering that a substantial amount of moisture in plant body (Bi et al.,
423 2009) was discharged during the process of straw combustion, the occurrence of
424 phenolic dimers might indicate that the aqueous phase reactions played an important
425 role in the formation and evolution of emitted aerosol organic composition.

426 Typical hydroxylated species such as, e.g., $C_2H_2O_4$, $C_6H_6O_2$, $C_7H_6O_3$, $C_7H_8O_3$, were
427 also found in the samples from photooxidation of both phenols and the WSBA samples.

The comparison of the photochemical products from phenols and the WSBA samples revealed their significant difference, pointing to the importance of studying real aerosol samples against the laboratory model compounds. However, evaluating the model compounds as proxy of real aerosol samples is always helpful as a reference. To this end, it is worth noting that potentially other phenols and methoxyphenols (e.g., acetosyringone, vanillin) that dissolve into cloud, fog droplets or aerosol liquid water can be photochemically transformed and contribute to the SOA formation (Vione et al., 2019, Zhou et al., 2019).

3.4 Photolysis of WSOC extracts from WSBA samples

Although the direct photolysis was performed on present WSOC extracts from WSBA samples in presence of simulated sunlight irradiation without adding any oxidants, the photooxidation process still occurred since the particle extracts were very likely to include various oxidants, e.g., singlet molecular oxygen ($^1O_2$), peroxides, hydroxyl radical (OH) or excited triplet state of organics produced under light excitation (Anastasio et al., 1997; Vione et al., 2006; Net et al., 2009; Net et al., 2010a; Bateman et al., 2011; Rossignol et al., 2014; Smith et al., 2014; Gómez Alvarez et al., 2012). In particular, the excited triplet state of aromatic carbonyls (e.g., 3, 4-dimethoxybenzaldehyde) (Net et al., 2010b) was found to be more efficient than OH radical to oxidize phenols and produce hydroxylated species (Smith et al., 2014., Yu et al., 2014). This photosensitized reaction is likely to play an important role in the WSOC evolution, due to high quantities of aromatic carbonyls present in the extracts of biomass burning aerosols.

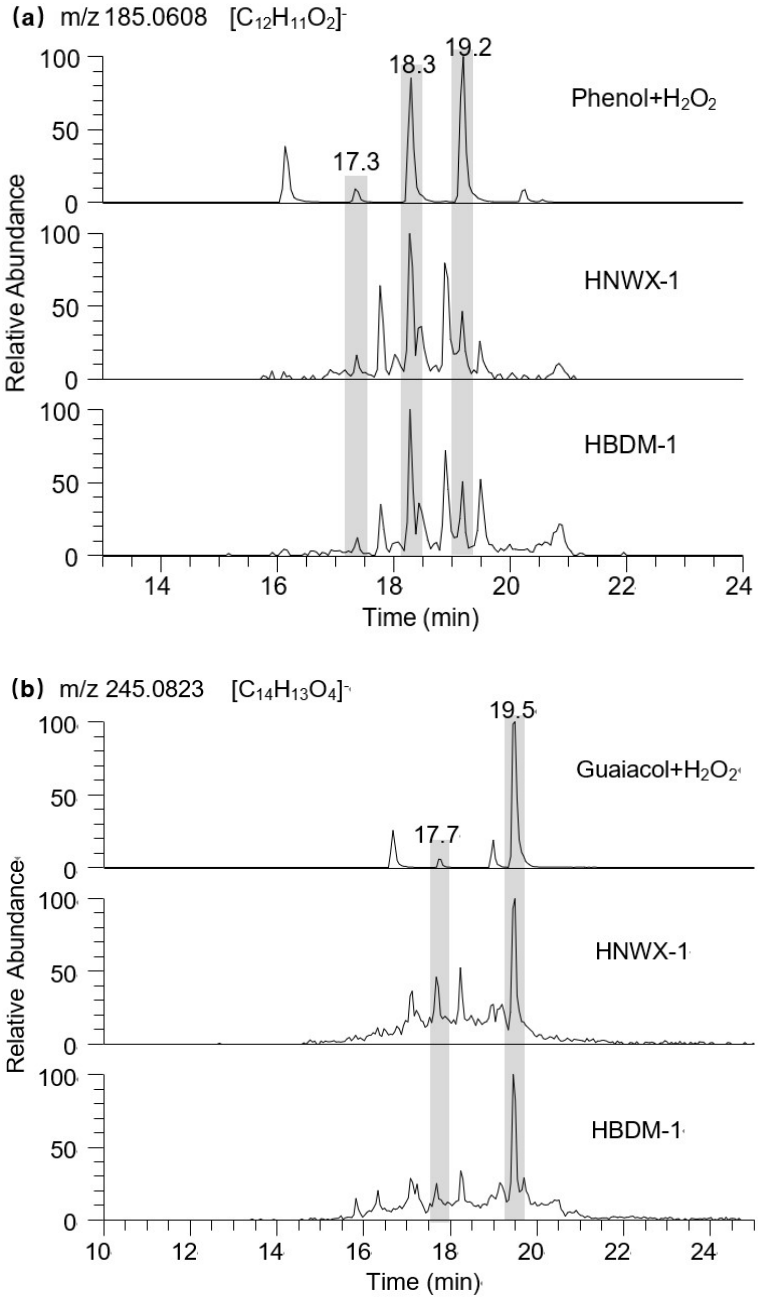

Figure 4. Extracted LC chromatograms of (a) m/z 185.0608 and (b) m/z 245.0823 in photochemical samples of phenols, HNWX-1, and HBDM-1, respectively.

The variation in peak abundance at unique retention times in the chromatogram could reflect the extent of evolution of WSOC molecules with accurate molecular weights, although no available standards were utilized for absolute quantification. The LC/ESI-HRMS monitors obviously changes in the molecular features of partial CHO species,

458 i.e., photodegradation of low oxygenated compounds and formation of high oxygenated
459 compounds. Table 1 lists the CHO compounds for which the LC peak intensities
460 significantly increased and decreased after the 12-hour photolysis.

461 **3.4.1 Photodegradation of low oxygenated compounds and formation of highly**
462 **oxygenated compounds**

463 As shown in Table 1, ion masses assigned with high unsaturated and low oxygenated
464 species (O/C $<$ 0.5) are prone to photodegradation, especially C_7-C_9 compounds
465 (possible aromatic species), which intensity decreased by nearly one order of magnitude.
466 For example, for m/z 123.0450 ($[C_7H_7O_2]^-$), as shown in Figure 5a, the peaks at RT 16.2
467 and 16.7 min in the LC chromatogram reduced in area by 95% after the 12-h irradiation.
468 Using a standard it was verified that both peaks did not belong to guaiacol (peak at
469 RT17.3 min), but they were also found within the products of guaiacol photooxidation,
470 suggesting that they might be isomers of guaiacol or aromatic dihydric alcohol.

471 The phenolic dimers ($C_{12}H_{10}O_2$ and $C_{14}H_{14}O_4$) as described above also exhibited a
472 decreasing tendency with almost complete disappearance after 12h direct photolysis.
473 Other species with relatively high MW ($\geqslant$ 200 Da) were also observed to be
474 decomposed, including m/z 251.0564 ($[C_{12}H_{11}O_6]^-$), 313.0724 ($[C_{17}H_{13}O_6]^-$), and
475 329.0674 ($[C_{17}H_{13}O_7]^-$) (Figure S7), although their initial abundance was not very high.

476 On the other hand, the solution acidity ($[H^+]$) of the particle extracts increase after
477 the 12-hour photolysis, similar to the observation on the photooxidation of phenols
478 (section 3.2) that resulted in the formation of oxygenated species. The solution acidity
479 ($[H^+]$) normalized by WSOC concentration ($[OC_{ws}]$) was increased with a variation of

480 $\Delta[H^+]/ [OC_{ws}] = (3.8 \pm 0.8) \times 10^{-7}$ mol mg C^{-1}, suggesting the formation of new acidic

481 substances.

482 **Table 1. *M/Z* with significant changes upon 12-h photolysis analyzed by LC/ESI-HRMS.**

Precursor (LC peak intensity decreases by ＞50%)			Product (LC peak intensity increases by ＞50%)		
Retention time, min	Measured *m/z*	Molecular formula	Retention time, min	Measured *m/z*	Molecular formula
16.2,16.7	123.04497	$C_7H_8O_2$	1.9	59.01362	$C_2H_4O_2$
13.9,14.5	129.05555	$C_6H_{10}O_3$	1.8	72.99291	$C_2H_2O_3$
14.6	131.07121	$C_6H_{12}O_3$	2.1	73.02928	$C_3H_6O_2$
14.6	133.02934	$C_8H_6O_2$	1.8	75.00856	$C_2H_4O_3$
15.9	135.04498	$C_8H_8O_2$	2.4	85.02930	$C_4H_6O_2$
13.7	137.02426	$C_7H_6O_3$	1.9, 4.4	87.04496	$C_4H_8O_2$
17.7	137.06063	$C_8H_{10}O_2$	1.9	88.98785	$C_2H_2O_4$
15.8	147.04504	$C_9H_8O_2$	1.9	89.02427	$C_3H_6O_3$
17.2	149.06062	$C_9H_{10}O_2$	2.2	99.00857	$C_4H_4O_3$
19.0	151.07634	$C_9H_{12}O_2$	2.5	129.01917	$C_5H_6O_4$
16.8	161.06068	$C_{10}H_{10}O_2$	2.0	145.01407	$C_5H_6O_5$
16.2	165.05559	$C_9H_{10}O_3$	1.9	147.02971	$C_5H_8O_5$
14.9	167.07129	$C_9H_{12}O_3$	14.9	155.03482	$C_7H_8O_4$
15.1	181.05048	$C_9H_{10}O_4$	15.1	169.01411	$C_7H_6O_5$
17.3	191.03498	$C_{10}H_8O_4$	16.4	183.02980	$C_8H_8O_5$
16.2	195.06622	$C_{10}H_{12}O_4$			
18.6	207.06635	$C_{11}H_{12}O_4$			

483 The photochemical processing has led to an increased formation of low MW

484 compounds (e.g., C_2-C_5 species), with a relatively high O/C. For example, the C_2

485 compounds, including $[C_2H_1O_3]^-$, $[C_2H_3O_3]^-$, $[C_2H_3O_2]^-$, and $[C_2H_1O_4]^-$ (Figure S8),

486 which may correspond to glyoxylic acid, glycolic acid, acetic acid, and oxalic acid,

487 respectively, were likely to be formed via oxidation pathway of several water-soluble

488 molecules with photochemical reactivity (e.g., glyoxal (Carlton et al., 2007; Lim et al.,

489 2010), methylglyoxal (Altieri et al., 2008; Lim et al., 2010), pyruvic acid (e.g. Grgic et

490 al., 2010; Griffith et al., 2013; Reed Harris et al., 2014; Rapf et al., 2017; Eugene and

Guzman, 2017, Mekic et al., 2018; Mekic et al., 2019), phenols (Sun et al., 2010), etc). The presence of these highly oxygenated compounds that possibly contain acidic groups (e.g., –COOH and –OH) undoubtedly contributed to the increase of the solution acidity. Higher levels of other highly oxygenated species such as $[C_3H_5O_3]^-$, $[C_4H_7O_2]^-$, $[C_5H_5O_5]^-$ and $[C_5H_7O_5]^-$ were also observed (Figure S9).

To identify the impact of photolysis on the evolution of specific WSOC, the ions of $[C_7H_7O_n]^-$ in the HBDM-1 sample with significant variation were chosen as representative cases for description. The relative intensity of $[C_7H_7O_2]^-$ and $[C_7H_7O_3]^-$ decreased dramatically, while the intensities of $[C_7H_7O_4]^-$, $[C_7H_7O_5]^-$ and $[C_7H_7O_6]^-$ increased with the irradiation time (Figure 5 shows only the variation of $[C_7H_7O_2]^-$ and $[C_7H_7O_4]^-$ as an example). It seems reasonable that the possible hydroxylation of $[C_7H_7O_2]^-$ and $[C_7H_7O_3]^-$ might contribute to the formation of $[C_7H_7O_5]^-$ and $[C_7H_7O_6]^-$. Although we could not verify this hypothesis, the formed oxidized species undoubtedly have a high O/C which highlights the possibility of this reaction pathway.

3.4.2 Presentation of photochemically stable organic species

Some of the detected organic species seemed to exhibit a good photochemical stability, as their relative intensities only slightly decreased (＜10%) after 12h light irradiation. The m/z 161.0454 ($[C_6H_9O_5]^-$) presented two prominent peaks at RT1.9 and 2.4 min (Figure S10). The peak at RT 2.4 min was further confirmed with a standard compound to be levoglucosan, a typical tracer of biomass burning aerosols with a high photochemical stability in atmospheric aerosols (Hu et al., 2013). The relatively good photochemical stability was also observed for some C_6 homolog compounds, such as

513 $[C_6H_7O_6]^-$, $[C_6H_9O_6]^-$, and $[C_6H_{11}O_6]^-$. Some other oxygenated species, such as

514 $[C_3H_3O_3]^-$, $[C_4H_5O_4]^-$, $[C_3H_3O_4]^-$, and $[C_4H_5O_5]^-$ remained relatively stable, as well.

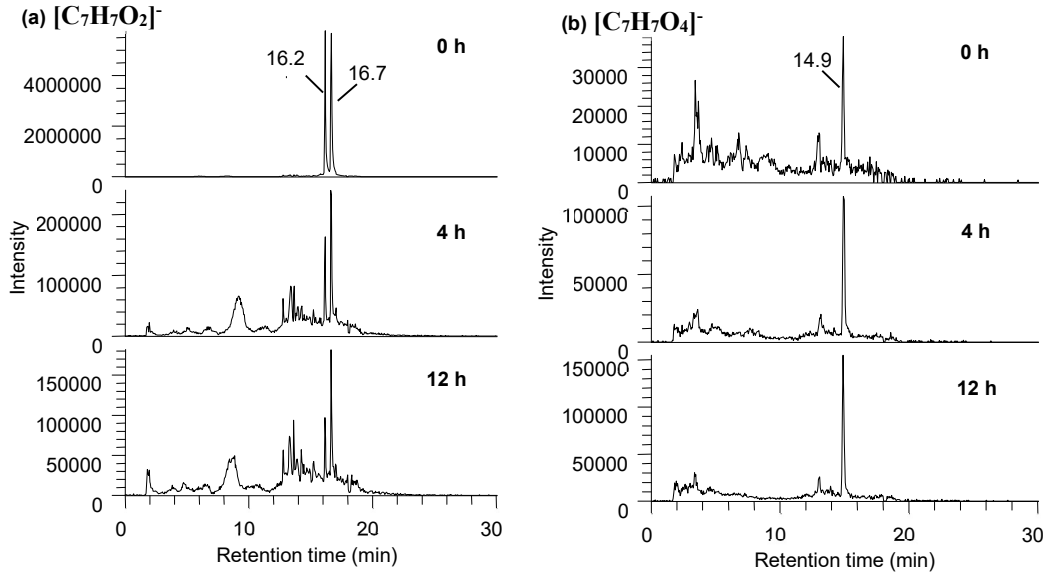

515

516 **Figure 5. Extracted LC chromatograms from HBDM-1 of (a) $[C_7H_7O_2]^-$ and (b) $[C_7H_7O_4]^-$ at**
517 **different photolytic stages of 0, 4, and 12 h.**

518 Regarding the CHON compounds, only small variation of the chromatogram peaks,

519 was observed for most of the detected species. In particular, several species with low

520 O/C decreased by less than 30%, e.g., m/z 94.0297 ($[C_5H_4ON]^-$, RT 7.1 min), and

521 120.0453 ($[C_7H_6ON]^-$, RT12.2 min). Some compounds seem photochemically very

522 stable as the variation of their peak intensities was less than 10 % upon light irradiation

523 of the samples, e.g., m/z 118.0297 ($[C_7H_4ON]^-$, RT16.6 and 17.1 min), 146.0246

524 ($[C_8H_4O_2N]^-$, RT14.4 min), and 190.0510 ($[C_{10}H_8O_3N]^-$, RT17.8 min). However, the

525 intensities of the ion masses with relatively higher degree of oxygenation was found to

526 increase substantially (>50%), e.g., m/z 162.0195 ($[C_8H_4O_3N]^-$, RT 17.2 min), 198.0408

527 ($[C_8H_8O_5N]^-$, RT 18.0 min), and 242.1763 ($[C_{13}H_{24}O_3N]^-$, RT 17.9 min). The

528 photochemical stability of some compounds may be ascribed to their low

concentrations, or the light-shielding effect from other light-absorbing species.

Another intriguing finding was that different structural isomers with the same molecular mass might have exhibited different fates upon prolonged light irradiation of the samples. For example, the intensity of the peak at m/z 165.0405 ($[C_5H_9O_6]^-$) decreased when it was eluted at 4.9 min, but increased at RT 1.8 min, with the irradiation time (Figure S11). A simultaneous degradation and formation among isomers of some CHON ion masses upon prolonged light irradiation, was also observed, as was the case for the CHO compounds. For example, the m/z 108.0453 assigned to $[C_6H_6ON]^-$, might include hydroxy and amino groups on the phenyl ring to present three possible isomers (Figure S12). During photolytic processing, the intensity of the peak at RT 3.2 min increased dramatically, while there was a clear decreasing tendency of the peak intensity at RT 5.5 and 12.5 min, which was suggestive of possible isomerization among these isomers. Other ion masses that exhibited possible isomerization included m/z 122.0610 ($[C_7H_8ON]^-$), 132.0454 ($[C_8H_6ON]^-$), 134.0245 ($[C_7H_4O_2N]^-$), 136.0403 ($[C_7H_6O_2N]^-$), 138.0559 ($[C_7H_8O_2N]^-$), 144.0453 ($[C_9H_6ON]^-$), and 152.0352 ($[C_7H_6O_3N]^-$).

3.4.3 Comparison of time-profile mass spectra of CHO composition in WSOC extracts from WSBA samples

Since the LC method just separated a fraction of polar compounds, we tentatively utilized the change of HRMS to gain more comprehensive information about the WSOC evolution. We compared the time-profile (0, 4, and 12h) mass spectra with each other, based on the assumption of same interference from inorganic species, and the good

551 reproducibility and stability for Orbitrap MS operated under the same instrumental
552 parameters (the RSD of TIC intensity within 5%). It is well known that ESI mass
553 spectral abundances are influenced by the solution composition, concentration of
554 analytes and instrumental factors (Bateman et al., 2011); hence, it is quite challenging
555 to directly quantify the absolute concentration levels of the complex mixtures. Despite
556 that, the photochemical degradation of WSOC compounds and corresponding
557 formation of organic compounds can be well described by the variation of signal
558 intensity from mass spectrometry. The average O/C and H/C for CHO compounds were
559 from 0.38 ± 0.02 to 0.44 ± 0.02 and 1.24 ± 0.03 to 1.26 ± 0.01, respectively, as the
560 irradiation time extended from 0 to 12h. The comparison of these time-profile mass
561 spectra indicates that the 12-hour photolysis resulted in a significant reduction of 28 ±
562 11% in the total ion abundance (S/N). Since the photolysis induced changes in
563 abundance for most of the CHO compounds, we also calculated the intensity (S/N)-
564 weighted average O/C (O/C_w) and H/C (H/C_w) (Bateman et al., 2011; Romonosky et
565 al., 2015) with values ranging from 0.45 ± 0.03 to 0.53 ± 0.06 and from 1.32 ± 0.09 to
566 1.40 ± 0.11, respectively. After the 12-h photolysis, both average H/C and H/C_w values
567 slightly increased, compared to the samples prior to irradiation, however, both average
568 O/C and O/C_w values have increased more distinctly, indicating an elevation in
569 oxidation degree of bulk extract composition. This phenomenon could be partly
570 reflected on the LC-HRMS observation, i.e. formation of highly oxygenated species
571 and the consumption of low oxygenated compounds. In our previous study, the UV-VIS
572 measurements revealed that the 12-h photochemical evolution leads to a modification

of absorptive properties for WSBA extracts (e.g., photo-bleaching at wavelengths below 380 nm and photo-enhancement above 380 nm) (Cai et al., 2018), which might be partially linked to present findings about molecular functionalization, e.g., hydroxylation facilitating a red shift for light absorbing wavelengths.

4 CONCLUSIONS

This study was focused on the effect of direct photolysis on the molecular composition of actual WSOC extracted from field straw-burning aerosol. The phenol dimer (m/z 185.0608) and guaiacol dimer (m/z 245.0823), or their isomers generated from laboratory aqueous-phase photooxidation of phenol and guaiacol were also observed in present field WSBA samples, suggesting that the aqueous phase reaction might contribute to the formation of emitted biomass burning aerosols. The laboratory observation on aqueous photochemistry of phenols indicated that those phenolic compounds in real biomass burning aerosols would likely have potential to experience similar evolution to form various oxygenated compounds under relevant atmospheric water conditions. The direct photolysis on the molecular composition of WSOC extracts from WSBA samples were performed to gain more insight into the evolution of aerosol composition. Because the extract composition was very complex, the techniques (ESI-HRMS and LC/ESI-HRMS) used in this study, although advanced still had limitations in monitoring the modification of molecular composition, especially for determining the potential formation of compounds present at low concentrations or compounds that were poorly ionized. However, a series of polar molecules were identified that changed their molecular composition via photochemical aging. In particular, the degradation of

low oxygenated compounds with strong photochemical reactivity and the formation of high oxygenated compounds might directly result in an increasing O/C in WSOC composition, which was likely linked to the modification of light-absorbing characteristics for extracts in previous study. This finding indicates that the water soluble organic fraction of field combustion-derived aerosols has the potential to form more oxidized organic matter, which might contribute to the highly oxygenated nature of atmospheric organic aerosols. Further studies focused on the photochemical evolution of WSOC composition will be performed in the future, including enlarging measurements on compound species (e.g., applying positive ESI-HRMS), identifying biomarkers and evaluating their role in photochemical processes.

AUTHOR CONTRIBUTION

Jing Cai and Zhiqiang Yu designed the experiments, and Jing Cai and Xiangying Zeng carried them out. Guorui Zhi provided the straw-burning aerosol samples, Zhiqiang Yu and Sasho Gligorovski helped to perform the analysis of light irradiation and editing the manuscript. Guoying Sheng, Xinming Wang and Ping'an Peng provided some technical consultations about organic chemistry. Jing Cai prepared the manuscript with contributions from all co-authors.

ACKNOWLEDGMENTS

This study was financially supported by the National Key Technology Research and Development Program of the Ministry of Science and Technology of China (2014BAC22B04), the National Natural Science Foundations of China (41225013,

41530641, 41373131, 41773131, and 41977187) and the Science and Technology Project of Guangdong Province, China (2014B030301060). We are grateful to Guangdong Foundation for Program of Science and Technology Research, Grant N°: 2017B030314057.

REFERENCES

Altieri, K. E., Seitzinger, S. P., Carlton, A. G., Turpin, B. J., Klein, G. C. and Marshall, A. G.: Oligomers formed through in-cloud methylglyoxal reactions: Chemical composition, properties, and mechanisms investigated by ultra-high resolution FT-ICR mass spectrometry. Atmospheric Environment, 42, 1476-1490, 2008.

Altieri, K. E., Turpin, B. J. and Seitzinger, S. P.: Oligomers, organosulfates, and nitrooxy organosulfates in rainwater identified by ultra-high resolution electrospray ionization FT-ICR mass spectrometry, Atmospheric Chemistry and Physics, 9, 2533-2542, 2009a.

Altieri, K. E., Turpin, B. J. and Seitzinger, S. P.: Composition of Dissolved Organic Nitrogen in Continental Precipitation Investigated by Ultra-High Resolution FT-ICR Mass Spectrometry, Environmental Science & Technology, 43, 6950-6955, doi: 10.1021/es9007849, 2009b.

Anastasio, C., Faust, B. C. and Rao, C. J.: Aromatic carbonyl compounds as aqueous-phase photochemical sources of hydrogen peroxide in acidic sulfate aerosols, fogs, and clouds .1. Non-phenolic methoxybenzaldehydes and methoxyacetophenones with reductants (phenols), Environmental Science & Technology, 31, 218-232, 1997.

Bateman, A. P., Nizkorodov, S. A., Laskin, J. and Laskin, A.: Photolytic processing of secondary organic aerosols dissolved in cloud droplets, Physical Chemistry Chemical Physics,13, 12199-12212, doi: 10.1039/c1cp20526a, 2011.

Bi, Y., Gao, C., Wang, Y., and Li, B.: Estimation of straw resources in China, Transactions of the Chinese Society of Agricultural Engineering, 25, 211-217, 2009.

Boone, E. J., Laskin, A., Laskin, J., Wirth, C., Shepson, P. B., Stirm, B. H. and Pratt, K. A.: Aqueous Processing of Atmospheric Organic Particles in Cloud Water Collected via Aircraft Sampling, Environmental Science & Technology,49, 8523-8530, doi: 10.1021/acs.est.5b01639, 2015.

643 Cai, J., Zhi, G., Yu, Z., Nie, P., Gligorovski, S., Zhang, Y., Zhu, L., Guo, X., Li, P., He, T., He, Y.,
644 Sun, J. and Zhang, Y.: Spectral changes induced by pH variation of aqueous extracts derived from
645 biomass burning aerosols: Under dark and in presence of simulated sunlight irradiation,
646 Atmospheric Environment, 185, 1-6, doi: 10.1016/j.atmosenv.2018.04.037. 2018.
647 Cappiello, A., De Simoni, E., Fiorucci, C., Mangani, F., Palma, P., Trufelli, H., Decesari, S., Facchini, M.
648 C. and Fuzzi, S.: Molecular characterization of the water-soluble organic compounds in fogwater
649 by ESIMS/MS, Environmental Science & Technology, 37, 1229-1240, doi: 10.1021/es0259990,
650 2003.
651 Chang, J. L. and Thompson, J. E.: Characterization of colored products formed during irradiation of
652 aqueous solutions containing H2O2 and phenolic compounds, Atmospheric Environment, 44, 541-
653 551, doi: 10.1016/j.atmosenv.2009.10.042, 2010.
654 Carlton, A. G., Turpin, B. J.. Altieri, K. E., Seitzinger, S.. Reff, A., Lim, H-J. and Ervens, B.: Atmospheric
655 oxalic acid and SOA production from glyoxal: Results of aqueous photooxidation experiments.
656 Atmospheric Environment, 41, 7588–7602, 2007.
657 Collett, J.L., Hoag, K.J., Sherman, D.E., Aaron Bator; Richards, W.L. Spatial and temporal variations in
658 San Joaquin Valley fog chemistry, Atmospheric Environment, 33 (1), 129-140, 1998.Daumit, K. E.,
659 Carrasquillo, A. J., Hunter, J. F. and Kroll, J. H.: Laboratory studies of the aqueous-phase oxidation
660 of polyols: submicron particles vs. bulk aqueous solution, Atmospheric Chemistry and Physics,14,
661 10773-10784, doi: 10.5194/acp-14-10773-2014, 2014.
662 Duarte, R. M. B. O., Santos, E. B. H., Pio, C. A. and Duarte, A. C.: Comparison of structural features of
663 water-soluble organic matter from atmospheric aerosols with those of aquatic humic substances,
664 Atmospheric Environment,41, 8100-8113, doi: 10.1016/j.atmosenv.2007.06.034, 2007.
665 Eugene, A. J. and Guzman, M. I. Reactivity of Ketyl and Acetyl Radicals from Direct Solar Actinic
666 Photolysis of Aqueous Pyruvic Acid. Journal of Physical Chemistry A , 121, 2924−2935, 2017.
667 Fahey, K. M., Pandis, S. N.. Collett, J. L. and Herckes, P. The influence of size-dependent droplet
668 composition on pollutant processing by fogs, Atmospheric Environment, 39(25), 4561-4574, 2005.
669 Fine, P. M., Cass, G. R. and Simoneit, B. R. T.: Chemical characterization of fine particle emissions from
670 fireplace combustion of woods grown in the northeastern United States, Environmental Science &
671 Technology,35, 2665-2675, 2001.
672 Fu, P. Q., Kawamura, K., Chen, J., Qin, M. Y., Ren, L. J., Sun, Y. L., Wang, Z. F., Barrie, L. A., Tachibana,

673 E., Ding, A. J. and Yamashita, Y.: Fluorescent water-soluble organic aerosols in the High Arctic
674 atmosphere, Scientific Reports,5, 2015.
675 Gilardoni, S., Massoli, P., Paglione, M., Giulianelli, L., Carbone, C., Rinaldi, M., Decesari, S., Sandrini,
676 S., Costabile, F., Gobbi, G. P., Pietrogrande, M. C., Visentin, M., Scotto, F., Fuzzi, S. and Facchini,
677 M. C.: Direct observation of aqueous secondary organic aerosol from biomass-burning emissions,
678 Proceedings of the National Academy of Sciences of the United States of America,113, 10013-
679 10018, 2016.
680 Gómez Alvarez, E., Wortham, H., Strekowski, R., Zetzsch, C., S. Gligorovski,S.: Atmospheric photo-
681 sensitized heterogeneous and multiphase reactions: From outdoors to indoors, Environmental
682 Science & Technology, 46, 1955-1963, 2012.
683 Graham, B., Mayol-Bracero, O. L., Guyon, P., Roberts, G. C., Decesari, S., Facchini, M. C., Artaxo, P.,
684 Maenhaut, W., Koll, P. and Andreae, M. O.: Water-soluble organic compounds in biomass burning
685 aerosols over Amazonia-1. Characterization by NMR and GC-MS, Journal of Geophysical
686 Research-Atmospheres,107, doi: 10.1029/2001jd000336, 2002.
687 Grgic, I., Nieto-Gligorovski, L.I., Net, S., Temime-Roussel, B., Gligorovski, S. and Wortham, H.: Light
688 induced multiphase chemistry of gas-phase ozone on aqueous pyruvic and oxalic acids, Physical
689 Chemistry Chemical Physics, 12, 698-707, 2010.
690 Griffith, E. C., Carpenter, B. K., Shoemaker, R. K. and Vaida, V.: Photochemistry of aqueous pyruvic
691 acid, Proceedings of the National Academy of Sciences of the United States of America,110, 11714-
692 11719, doi: 10.1073/pnas.1303206110, 2013.
693 Hu, Q., Xie, Z., Wang, X., Hui Kang, H. and Zhang, P.: Levoglucosan indicates high levels of biomass
694 burning aerosols over oceans from the Arctic to Antarctic, Scientific Reports, 3, 2013.
695 Kitanovski, Z., Cusak, A., Grgic, I. and Claeys, M.: Chemical characterization of the main products
696 formed through aqueous-phase photonitration of guaiacol, Atmospheric Measurement Techniques,7,
697 2457-2470, doi: 10.5194/amt-7-2457-2014, 2014.
698 Kroll, J. H., Donahue, N. M., Jimenez, J. L., Kessler, S. H., Canagaratna,M. R., Wilson, K. R., Altieri, K.
699 E., Mazzoleni, L. R.,Wozniak, A. S., Bluhm, H., Mysak, E. R., Smith, J. D., Kolb,C. E., and Worsnop,
700 D. R.: Carbon oxidation state as a metricfor describing the chemistry of atmospheric organic aerosol,
701 Nat. Chem. Biol., 3, 133–139, 2011.
702 Kourtchev, I., Fuller, S., Aalto, J., Ruuskanen, T. M., McLeod, M. W., Maenhaut, W., Jones, R., Kulmala,

703 M. and Kalberer, M.: Molecular Composition of Boreal Forest Aerosol from Hyytiala, Finland,
704 Using Ultrahigh Resolution Mass Spectrometry, Environmental Science & Technology, 47, 4069-
705 4079, doi: 10.1021/es3051636, 2013.
706 Kourtchev, I., Godoi, R. H. M., Connors, S., Levine, J.G., Archibald1, A.T., Godoi, A. F. L., Paralovo,
707 S.L., Barbosa, C. G. G.,Souza, R. A. F., Manzi, A. O., Seco, R.,Sjostedt, S., Park, J. H., Guenther
708 A., Kim, S., Smith, J., Martin, S. T., and Kalberer, M.: Molecular composition of organic aerosols
709 in central Amazonia:,an ultra-high-resolution mass spectrometry study, Atmospheric Chemistry
710 and Physics, 16, 11899–11913, 2016.
711 Krivacsy, Z., Hoffer, A., Sarvari, Z., Temesi, D., Baltensperger, U., Nyeki, S., Weingartner, E., Kleefeld,
712 S. and Jennings, S. G.: Role of organic and black carbon in the chemical composition of atmospheric
713 aerosol at European background sites, Atmospheric Environment, 35, 6231-6244, 2001.
714 Laskin, A., Smith, J. S. and Laskin, J.: Molecular Characterization of Nitrogen-Containing Organic
715 Compounds in Biomass Burning Aerosols Using High-Resolution Mass Spectrometry,
716 Environmental Science & Technology, 43, 3764-3771, doi: 10.1021/es803456n, 2009.
717 Lavi,A.,Lin, P.,Bhaduri, B., Carmieli, R., Laskin, A. andRudich Y.: Characterizationof light-absorbing
718 oligomersfrom reactionsof phenolic compoundsandFe(III), Earth and Space Chemistry, 1, 637-646,
719 2017.
720 Lee, A. K. Y., Herckes, P., Leaitch, W. R., Macdonald, A. M. and Abbatt, J. P. D.: Aqueous OH oxidation
721 of ambient organic aerosol and cloud water organics: Formation of highly oxidized products,
722 Geophysical Research Letters, 38, 2011.
723 Lim, Y. B., Tan, Y., Perri, M. J., Seitzinger, S. P. and Turpin, B. J.: Aqueous chemistry and its role in
724 secondary organic aerosol (SOA) formation, Atmospheric Chemistry and Physics, 10, 10521-10539,
725 doi: 10.5194/acp-10-10521-2010, 2010.
726 Lim, Y. B. and Turpin, B. J.: Laboratory evidence of organic peroxide and peroxyhemiacetal formation
727 in the aqueous phase and implications for aqueous OH, Atmospheric Chemistry and Physics, 15,
728 12867-12877, doi: 10.5194/acp-15-12867-2015, 2015.
729 Lin, P., Rincon, A. G., Kalberer, M. and Yu, J. Z.: Elemental Composition of HULIS in the Pearl River
730 Delta Region, China: Results Inferred from Positive and Negative Electrospray High Resolution
731 Mass Spectrometric Data, Environmental Science & Technology, 46, 7454-7462, doi:
732 10.1021/es300285d, 2012a.

Lin, P., Yu, J. Z., Engling, G. and Kalberer, M.: Organosulfates in Humic-like Substance Fraction Isolated from Aerosols at Seven Locations in East Asia: A Study by Ultra-High-Resolution Mass Spectrometry, Environmental Science & Technology, 46, 13118-13127, doi: 10.1021/es303570v, 2012b.

Mayol-Bracero, O. L., Guyon, P., Graham, B., Roberts, G., Andreae, M. O., Decesari, S., Facchini, M. C., Fuzzi, S. and Artaxo, P.: Water-soluble organic compounds in biomass burning aerosols over Amazonia - 2. Apportionment of the chemical composition and importance of the polyacidic fraction, Journal of Geophysical Research-Atmospheres,107, doi: 10.1029/2001jd000522, 2002.

McNeill, V. F.: Aqueous Organic Chemistry in the Atmosphere: Sources and Chemical Processing of Organic Aerosols, Environmental Science & Technology, 49, 1237-1244, 2015.

Mekic, M., Loisel, G., Zhou, W.,Jiang, B.,Vione, D., Gligorovski, S.: Ionic strength effects on the reactive uptake of ozone on aqueous pyruvic acid: Implications for air-sea ozone deposition, Environmental Science and Technology, 52, 12306–12315,2018.

Mekic, M., Liu, J., Zhou, W., Loisel, G., Cai, J., He, T., Jiang, B., Yu, Z., Lazarou, Y. G., Li, X., Brigante, M., Vione, D., Gligorovski, S.: Formation of highly oxygenated multifunctional compounds from cross-reactions of carbonyl compounds in the atmospheric aqueous phase, Atmospheric Environment, 219, 117046, 2019.

Net, S., Nieto-Gligorovski,L.,Gligorovski, S., Temime-Rousell, B., Barbati, S., Lazarou, Y. G., and Wortham,H.: Heterogeneous light induced ozone processing on the organic coatings in the atmosphere, Atmospheric. Environment, 43, 1683-1692, 2009.

Net,S., Nieto-Gligorovski, L., Gligorovski, S., and Wortham, H.: Heterogeneous ozonation kinetics of 4-phenoxyphenol in presence of photosensitizer, Atmospheric Chemistry and Physics, 10, 1545-1554, 2010b.

Net, S., Gligorovski, S., and Wortham, H.: Light-induced heterogeneous ozone processing on organic coated particles: Kinetics and condensed-phase products, Atmospheric Environment, 44, 3286-3294, 2010b.

Nguyen, T. B., Lee, P. B., Updyke, K. M., Bones, D. L., Laskin, J., Laskin, A. and Nizkorodov, S. A.: Formation of nitrogen- and sulfur-containing light-absorbing compounds accelerated by evaporation of water from secondary organic aerosols, Journal of Geophysical Research-Atmospheres, 117, doi: 10.1029/2011jd016944, 2012.

763 Ofner, J., Krueger, H. U., Grothe, H., Schmitt-Kopplin, P., Whitmore, K. and Zetzsch, C.: Physico-
764 chemical characterization of SOA derived from catechol and guaiacol - a model substance for the
765 aromatic fraction of atmospheric HULIS, Atmospheric Chemistry and Physics, 11, 1-15, doi:
766 10.5194/acp-11-1-2011, 2011.
767 Petzold, A., Kopp, C., Niessner, R., 1997. The dependence of the specific attenuation cross-section on
768 black carbon mass fraction and particle size. Atmopheric Environment, 31, 661-672, 1997.
769 Prasse, C., Ford, B., Nomura, D.K. and Sedlak, D.L.: Unexpected transformation of dissolved phenols
770 to toxic dicarbonyls by hydroxyl radicals and UV light, https://doi.org/10.1073/pnas.1715821115,
771 2018.
772 Rapf, R. J., Perkins, R. J., Carpenter, B. K. and Vaida, V.: Mechanistic Description of Photochemical
773 Oligomer Formation from Aqueous Pyruvic Acid. Journal of Physical Chemistry A, 121, 4272−4282,
774 2017.
775 Reed Harris, A. E., Ervens, B., Shoemaker, R. K., Kroll, J. A., Rapf, R. J., Griffith, E. C., Monod, A.,
776 Vaida, V.: Photochemical kinetics of pyruvic acid in aqueous solution. Journal of Physical
777 ChemistryA, 118 (37), 8505−8516, 2014.
778 Romonosky, D. E., Laskin, A., Laskin, J. and Nizkorodov, S. A.: High-Resolution Mass Spectrometry
779 and Molecular Characterization of Aqueous Photochemistry Products of Common Types of
780 Secondary Organic Aerosols, Journal of Physical Chemistry A, 119, 2594-2606, doi:
781 10.1021/jp509476r, 2015.
782 Rossignol, S., Aregahegn, K. Z., Tinel, L., Fine, L., Noziere, B. and George, C.: Glyoxal Induced
783 Atmospheric Photosensitized Chemistry Leading to Organic Aerosol Growth, Environmental
784 Science & Technology, 48, 3218-3227, 2014.
785 Simoneit, B. R. T.: Biomass burning - A review of organic tracers for smoke from incomplete combustion,
786 Applied Geochemistry,17, 129-162, doi: 10.1016/s0883-2927(01)00061-0, 2002.
787 Smith, J. D., Sio, V., Yu, L., Zhang, Q. and Anastasio, C.: Secondary Organic Aerosol Production from
788 Aqueous Reactions of Atmospheric Phenols with an Organic Triplet Excited State, Environmental
789 Science & Technology,48, 1049-1057, doi: 10.1021/es4045715, 2014.
790 Smith, J. S., Laskin, A. and Laskin, J.: Molecular Characterization of Biomass Burning Aerosols Using
791 High-Resolution Mass Spectrometry, Analytical Chemistry,81, 1512-1521, doi: 10.1021/ac8020664,
792 2009.

793 Smith, J. D., Kinney, H. and Anastasio, C.:Phenolic carbonyls undergo rapid aqueous photodegradation
794 to form low-volatility, light-absorbing products,Atmospheric environment, 126, 36-44, 2015.
795 Sun, Y. L., Zhang, Q., Anastasio, C. and Sun, J.: Insights into secondary organic aerosol formed via
796 aqueous-phase reactions of phenolic compounds based on high resolution mass spectrometry,
797 Atmospheric Chemistry and Physics, 10, 4809-4822, doi: 10.5194/acp-10-4809-2010, 2010.
798 Surratt, J. D., Gomez-Gonzalez, Y., Chan, A. W. H., Vermeylen, R., Shahgholi, M., Kleindienst, T. E.,
799 Edney, E. O., Offenberg, J. H., Lewandowski, M., Jaoui, M., Maenhaut, W., Claeys, M., Flagan, R.
800 C. and Seinfeld, J. H.: Organosulfate formation in biogenic secondary organic aerosol, Journal of
801 Physical Chemistry A, 112, 8345-8378, doi: 10.1021/jp802310p, 2008.
802 Surratt, J. D., Kroll, J. H., Kleindienst, T. E., Edney, E. O., Claeys, M., Sorooshian, A., Ng, N. L.,
803 Offenberg, J. H., Lewandowski, M., Jaoui, M., Flagan, R. C. and Seinfeld, J. H.: Evidence for
804 organosulfates in secondary organic aerosol, Environmental Science & Technology,41, 517-527, doi:
805 10.1021/es062081q, 2007.
806 Tong, H., Kourtchev, I., Pant, P., Keyte, I. J., O'Connor, I. P., Wenger, J. C., Pope, F. D., Harrison, R. M.
807 and Kalberer, M.: Molecular composition of organic aerosols at urban background and road tunnel
808 sites using ultra-high resolution mass spectrometry. Faraday Discussions, 189, 51–68, 2016.
809 Vione, D., Maurino, V., Minero, C., Pelizzetti, E., Harrison, M. A. J., Olariu, R. I. and Arsene, C.:
810 Photochemical reactions in the tropospheric aqueous phase and on particulate matter, Chemical
811 Society Reviews, 35, 441-453, 2006.
812 Vione, V., Albinet, A., Barsotti, F.,Mekic,M., Jiang, B.,Minero, C.,Brigante, M.,Gligorovski, S.:
813 Formation of substances with humic-like fluorescence properties, upon photoinduced
814 oligomerization of typical phenolic compounds emitted by biomass burning, Atmospheric
815 Environment, https://doi.org/10.1016/j.atmosenv.2019.03.005,2019.
816 Wang, X. K., Rossignol, S., Ma, Y., Yao, L., Wang, M. Y., Chen, J. M., George, C. and Wang, L.:
817 Molecular characterization of atmospheric particulate organosulfates in three megacities at the
818 middle and lower reaches of the Yangtze River, Atmospheric Chemistry and Physics, 16, 2285-2298,
819 2016.
820 Wang, X., Hayeck, N., Brüggemann, M., Yao, L., Chen, H., Zhang, C., Emmelin, C., Jianmin Chen, J.,
821 George, C. and Lin Wang, L. Chemical characteristics of organic aerosols in shanghai: A study by
822 ultrahigh-performance liquid chromatography coupled with Orbitrap mass spectrometry, Journal of

Geophysical Research-Atmospheres, 122 (11), 703–722, 2017.

Wozniak, A. S., Bauer, J. E., Sleighter, R. L., Dickhut, R. M. and Hatcher, P. G.: Technical Note: Molecular characterization of aerosol-derived water soluble organic carbon using ultrahigh resolution electrospray ionization Fourier transform ion cyclotron resonance mass spectrometry, Atmospheric Chemistry and Physics, 8, 5099-5111, 2008.

Xie, M. J., Mladenov, N., Williams, M. W., Neff, J. C., Wasswa, J. and Hannigan, M. P.: Water soluble organic aerosols in the Colorado Rocky Mountains, USA: composition, sources and optical properties, Scientific Reports, 6, 2016.

Yee, L. D., Kautzman, K. E., Loza, C. L., Schilling, K. A., Coggon, M. M., Chhabra, P. S., Chan, M. N., Chan, A. W. H., Hersey, S. P., Crounse, J. D., Wennberg, P. O., Flagan, R. C. and Seinfeld, J. H.: Secondary organic aerosol formation from biomass burning intermediates: phenol and methoxyphenols, Atmospheric Chemistry and Physics, 13, 8019-8043, 2013.

Yu, L., Smith, J., Laskin, A., Anastasio, C., Laskin, J. and Zhang, Q.: Chemical characterization of SOA formed from aqueous-phase reactions of phenols with the triplet excited state of carbonyl and hydroxyl radical, Atmospheric Chemistry and Physics, 14, 13801-13816, doi: 10.5194/acp-14-13801-2014, 2014.

Zhao, Y., Hallar, A. G. and Mazzoleni, L. R.: Atmospheric organic matter in clouds: exact masses and molecular formula identification using ultrahigh-resolution FT-ICR mass spectrometry, Atmospheric Chemistry and Physics, 13, 12343-12362, doi: 10.5194/acp-13-12343-2013, 2013.

Zhi, G., Chen, Y., Xue, Z., Meng, F., Cai, J., Sheng, G. and Fu, J.: Comparison of elemental and black carbon measurements during normal and heavy haze periods: implications for research, Environmental Monitoring and Assessment, 186, 6097-6106, doi: 10.1007/s10661-014-3842-2, 2014.

Zhou, W., Mekic, M., Liu, J., Loisel, G., Jin, B., Vione, D., Gligorovski, S.: Ionic strength effects on the photochemical degradation of acetosyringone in atmospheric deliquescent aerosol particles, AtmosphericEnvironment, 198, 83-88, 2019.